



**HAL**  
open science

## Superplasticity in Fine Grain Ti-6Al-4V Alloy: Mechanical Behavior and Microstructural Evolution

Laurie Despax, Vanessa Vidal, Denis Delagnes, Moukrane Dehmas, Morgane Geyer, Hiroaki Matsumoto, Vincent Velay

► **To cite this version:**

Laurie Despax, Vanessa Vidal, Denis Delagnes, Moukrane Dehmas, Morgane Geyer, et al.. Superplasticity in Fine Grain Ti-6Al-4V Alloy: Mechanical Behavior and Microstructural Evolution. ICSAM 2018 - 13th International Conference on Superplasticity in Advanced Materials, Aug 2018, St Petersburg, Russia. pp.137-143, 10.4028/www.scientific.net/DDF.385.137 . hal-01864428

**HAL Id: hal-01864428**

**<https://hal.science/hal-01864428>**

Submitted on 8 Feb 2020

**HAL** is a multi-disciplinary open access archive for the deposit and dissemination of scientific research documents, whether they are published or not. The documents may come from teaching and research institutions in France or abroad, or from public or private research centers.

L'archive ouverte pluridisciplinaire **HAL**, est destinée au dépôt et à la diffusion de documents scientifiques de niveau recherche, publiés ou non, émanant des établissements d'enseignement et de recherche français ou étrangers, des laboratoires publics ou privés.

# Superplasticity in Fine Grain Ti-6Al-4V Alloy: Mechanical Behavior and Microstructural Evolution

Laurie Despax<sup>1,a\*</sup>, Vanessa Vidal<sup>1,b</sup>, Denis Delagnes<sup>1,c</sup>, Moukrane Dehmas<sup>2,d</sup>, Morgane Geyer<sup>1,e</sup>, Hiroaki Matsumoto<sup>3,f</sup> and Vincent Velay<sup>1,g</sup>

<sup>1</sup>Institut Clément Ader (ICA), Université de Toulouse, CNRS, IMT Mines Albi, UPS, INSA, ISAE-SUPAERO, Campus Jarlard, 81013 Albi CT Cedex 09, France.

<sup>2</sup>CIRIMAT, Université de Toulouse, UPS-INP-CNRS, INP/ENSIACET, 4 allée Emile Monso, BP 44362, 31030 Toulouse Cedex 04, France.

<sup>3</sup>Department of Advanced Materials Science, Faculty of Engineering, Kagawa University, 2217-20 Hayashi-cho, Takamatsu, Kagawa 761-0396, Japan.

<sup>a</sup>laurie.despax@mines-albi.fr, <sup>b</sup>vvidal@mines-albi.fr, <sup>c</sup>denis.delagnes@mines-albi.fr,

<sup>d</sup>moukrane.dehmas@ensiacet.fr, <sup>e</sup>morgane.geyer@mines-albi.fr, <sup>f</sup>matsu\_h@eng.kagawa-u.ac.jp, <sup>g</sup>vincent.velay@mines-albi.fr

**Keywords:** Superplasticity, Titanium alloys, Ti-6Al-4V, Mechanical behavior, Texture,  $\beta$ -phase proportion.

**Abstract.** Titanium Ti-6Al-4V alloys are known to exhibit interesting superplastic properties for different conditions of temperature and strain rate, depending on the initial grain size. Even if superplasticity is generally explained in terms of grain boundary sliding (GBS) accompanied by several accommodation mechanisms, it appears that the micromechanisms of superplasticity are still controversial especially at the grain scale and even more at lower scale. These micromechanisms, involving microstructural evolution, depend also on the SPF conditions (temperature, strain rate and initial microstructure). In this study, the flow stress in the Ti-6Al-4V alloy is investigated for different strain rate and for temperature in the range of the  $\alpha/\beta$  transformation. The preferred orientation evolution of alpha phase grains for different percentage of deformation is studied for a non-optimal SPF regime ( $920^{\circ}\text{C}-10^{-4} \text{ s}^{-1}$ ) in order to highlight the microstructural evolution and so the deformation mechanisms involved. For that, mechanical interrupted test combined with Scanning Electron Microscopy (SEM) and Electron Back Scatter Diffraction (EBSD) are used.

## Introduction

Titanium alloys are widely used in structural application for their excellent properties such as high strength to weight ratio, low density and good corrosion resistance. Superplastic forming (SPF) is an expensive process requiring high temperatures and low strain rates. Several studies on titanium alloys deal with the decrease of its cost by improving the formability of materials [1] at lower temperature, in particular, using refined microstructure [2-3]. So the superplasticity is reached for a huge range of temperatures and strain rates as a function of microstructure. Our interest mainly concerns the two phase ( $\alpha+\beta$ ) Ti-6Al-4V alloy. For this alloy depending on the forming conditions, several stress-strain responses can be observed. Indeed as a function of the temperature, the phases in presence as well as their distribution can significantly change and so leading to different mechanism of deformation. The understanding of the deformation mechanisms involved during SPF are still a major issue. Indeed in the literature many mechanisms, as grain boundaries migration, grain boundaries sliding [4], dynamic recrystallization or dislocation slip, are reported.

Earlier studies on Ti-6Al-4V alloys showed, by in-situ observations [5], that the predominant mechanism at  $800^{\circ}\text{C}$  is the Grain Boundary Sliding (GBS) with in addition dislocation motion in  $\alpha$  grains leading to recrystallization. At  $900^{\circ}\text{C}$ , Alabort describes a mechanism of GBS completed by the motion of dislocations in  $\beta$  [5]. In this context, our study investigates the mechanical behavior and the microstructural evolution for a wide range of temperature ( $750^{\circ}\text{C}-920^{\circ}\text{C}$ ) and strain rates ( $10^{-2} \text{ s}^{-1}-10^{-4} \text{ s}^{-1}$ ) of a fine grain Ti-6Al-4V ( $d_{\alpha} = 3 \mu\text{m}$ ).

Moreover a specific attention is pay on the  $\beta$  phase fraction evolution in this temperature range. Then to assess the mechanisms involved under a non-optimal SPF condition, for which the  $\beta$  phase fraction is high, the grains orientation evolution is studied by using interrupted tensile tests at 920°C, with a strain rate of  $10^{-4} \text{ s}^{-1}$ . Then the effect of temperatures and the role of each phase can be discussed.

## Experimental

**Samples.** The material investigated is a Ti-6Al-4V alloy, in the form of sheet. The chemical composition of this alloy is about (in wt%) 6.25Al, 3.90V, 0.24Fe and balance titanium. The microstructure studied is a 3 mm thick sheet with an initial average  $\alpha$  grains size of 3  $\mu\text{m}$  (named hereafter as the starting microstructure SM). The microstructural characterization of the SM sample was done by Scanning Electron Microscopy (SEM) with image analysis, X-Ray Diffraction and Electron Back Scatter Diffraction (EBSD).

**Tensile tests at high temperature.** Tensile tests, along the rolling direction, with different temperatures and different strain rate were conducted, respectively in the range of 750°C-920°C and  $10^{-2} \text{ s}^{-1}$  and  $10^{-4} \text{ s}^{-1}$ , on dog bone specimen [6] according to the procedure presented by Velay [7]. Before each tests, the samples were held at temperature for about 20 min prior tensile loading. For the tensile tests at 870°C and 920°C argon atmosphere are used to limit the oxygen diffusion. After tensile tests, the cooling is done into the furnace. During this slow cooling a change in the grain size could probably occur and so the microstructure observed at room temperature is probably not representative of that at high temperature. In particular the  $\alpha$  grain size could be over-estimated. Interrupted tensile tests, at 920°C and with a strain rate of  $10^{-4} \text{ s}^{-1}$ , were also conducted to study more precisely the evolution of microstructure. The tensile tests were interrupted at 200%, 400% and 800% of strain. After interrupted tensile tests, the deformed SM specimen were cooled down in the furnace and prepared for EBSD measurement using standard metallographic technics. Note that the X0 axis, used in EBSD and in XRD, corresponds to the rolling direction of the Ti-6Al-4V sheet.

**Heat treatments.** To determine the volume fraction of  $\alpha$  (and so  $\beta$ ) as function of the temperature, several samples from the SM were heat treated for two hours with temperatures in the range of 700°C-920°C followed by water quenching. The heating rate selected was about 10°C per minutes to keep nearly the same conditions than tensile tests. The microstructure was studied with a SEM (NOVANOSEM 450) by using the backscattered electron (BSE) imaging mode associated by image analysis. In such conditions,  $\alpha$  and  $\beta$  appear respectively dark and white. For samples water quenched from temperatures included in the range of the  $\alpha \rightarrow \beta$  transformation, the martensitic  $\alpha'$  appears grey and lathlike. It is important to notice that this martensitic  $\alpha'$  observed at room temperature belongs to the  $\beta$  phase at high temperature as during the water quenching the  $\beta$  phase transforms into the fine martensitic structure.

## Results and Discussion

**Initial state characterization (SM).** Fig 1 shows the initial microstructure of the Ti-6Al-4V sheet studied. The microstructure consists of equiaxed grains slightly elongated along the RD of the hexagonal  $\alpha$  phase with a mean grain diameter of approximately 3  $\mu\text{m}$  decorated by the  $\beta$  phase. Texture measurements performed by X-rays diffraction indicate, in the  $\alpha$  phase, a strong rolling texture with basal poles  $\{0002\}$  tilted by  $\pm 25^\circ$  from the normal direction to the rolling direction (Fig. 1b). EBSD measurements (Fig. 1c) seems to show, in the  $\beta$  phase, the so-called « cube texture » for which the grains are oriented so that the  $\{001\}$  planes lie nearly parallel to the plane of the sheet and the  $\langle 100 \rangle$  directions are almost parallel to the rolling direction. Nevertheless, from EBSD measurements a very low statistics is obtained for the  $\beta$  phase. Thus it appears really difficult to clearly conclude on the initial texture of the  $\beta$  phase.

**Mechanical behavior.** Fig. 2 shows the curves obtained after tensile tests carried out at different temperature with different strain rate.

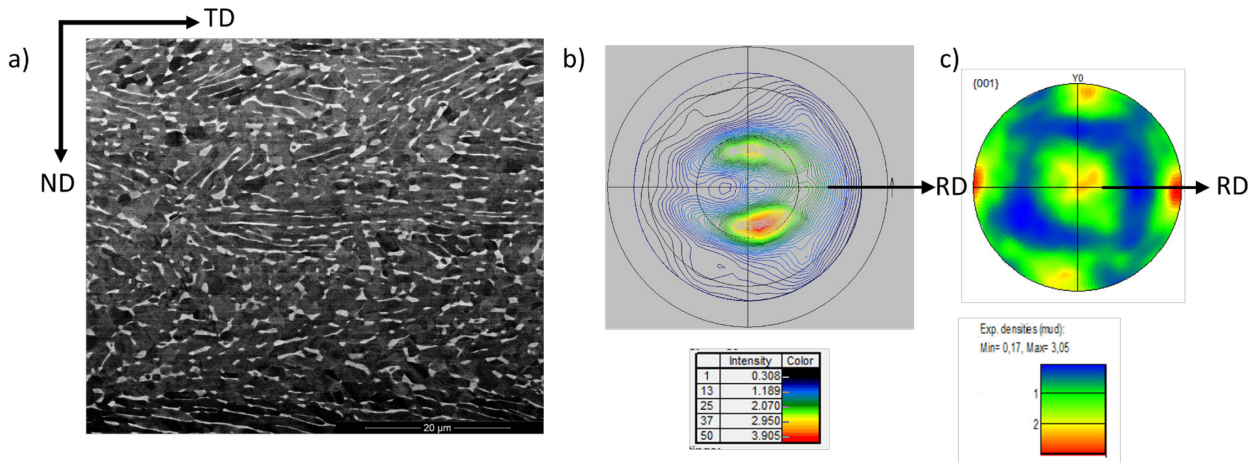


Fig. 1: Ti-6Al-4V initial state with  $\alpha$  grain (black) size about  $3 \mu\text{m}$  characterized by SEM (a). Incomplete (0002) pole figure measured by X-Ray Diffraction showing the initial texture of the  $\alpha$  phase in the SM titanium alloy (using an iso-lines presentation with normalized intensity values (b) representing the plan 0002 of the  $\alpha$  phase texture (b) and  $\{001\}$  pole figure measured by EBSD in the  $\beta$  phase (c).

The steady-state flow on stress-strain curve occurs due to superplastic flow. Fig. 2a, 2b and 2c shows the stress-strain curves obtained for the SM at respectively  $750^\circ\text{C}$ ,  $870^\circ\text{C}$  and  $920^\circ\text{C}$ . At  $750^\circ\text{C}$  and  $870^\circ\text{C}$ , experimental data are compared with computed data (lines) obtained using the mechanical model from Velay [7]. As detailed in Ref.7, an internal variable related to grain growth is introduced into the mechanical model through the viscous flow and the hardening. So by taking into account the grain growth (as revealed by SEM observations on Fig.3), computed and experimental data are in good agreement. In particular for high temperature and/or slow strain rate (long duration test), the strain hardening observed is well described by this model. For temperature lower than  $920^\circ\text{C}$ , if we assumed that the steady-state flow observed on stress-strain curve is due to grain boundary sliding (GBS), the hardening can be reasonably explained by the grain growth evolution [7].

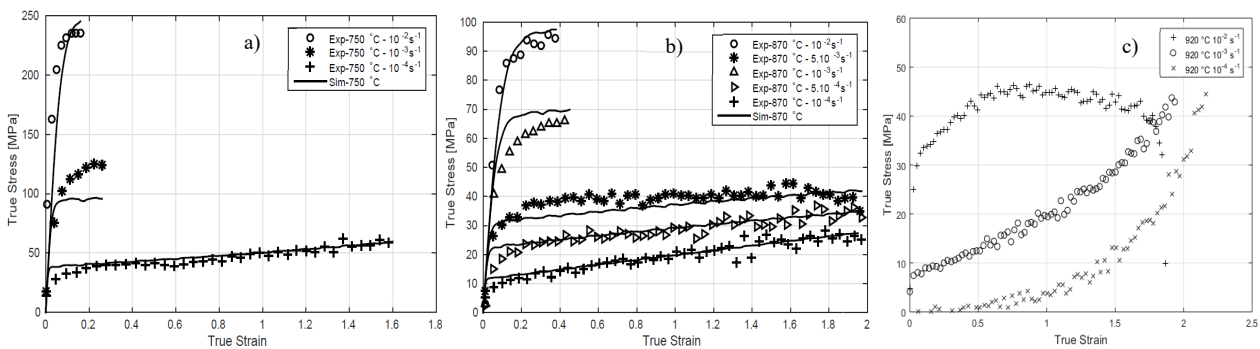


Fig. 2: Stress-strain for SM curves at  $750^\circ\text{C}$  (a),  $870^\circ\text{C}$  (b) and  $920^\circ\text{C}$  (c) for different strain rates. Experimental data (Symbols) are compared to computed stress-strain data (Lines) obtained using the mechanical model from Velay [7]. The note that a and b are from ref 7.

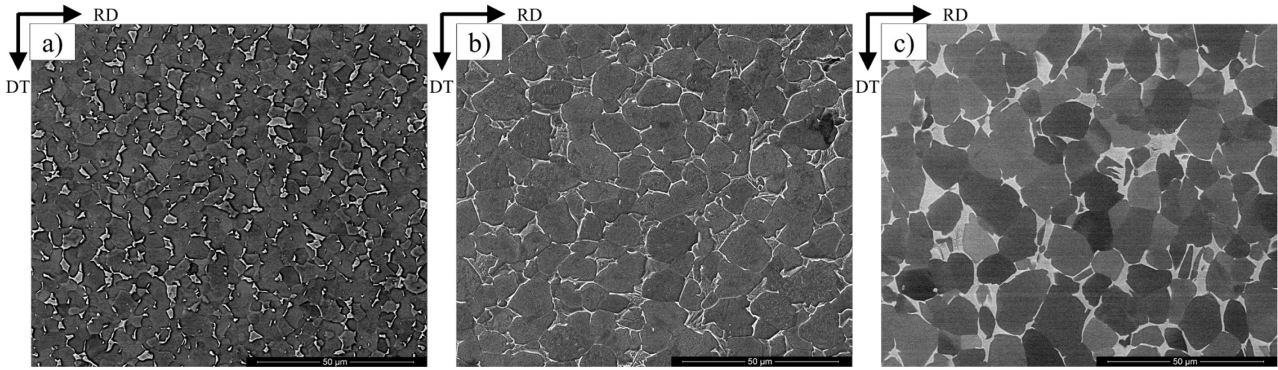


Fig. 3: Microstructural observations after superplastic testing with a strain rate about  $10^{-4} \text{ s}^{-1}$  at  $750^\circ\text{C}$  (a),  $870^\circ\text{C}$  (b) et  $920^\circ\text{C}$  (c) obtained after furnace cooling by SEM with CBS x1000.

At  $920^\circ\text{C}$  and with a fast strain rate of  $10^{-2} \text{ s}^{-1}$ , a peak flow stress followed by a steady-state flow then by a strain softening is observed. Note that this flow softening could be associated to dynamic recrystallization [8-9-10]. For higher strain rate ( $10^{-4}$  and  $10^{-3} \text{ s}^{-1}$ ), the flow behavior is completely different as a pronounced flow hardening is revealed on Fig. 2c. Meanwhile, at  $920^\circ\text{C}$ , the mechanical model taking into account the grain growth failed in the prediction of the stress-strain behavior. This revealed that not only the grain growth but other microstructural parameters could also play a role in the mechanisms of superplasticity. In particular, at this temperature the  $\beta$  phase fraction is higher than the  $\alpha$  phase fraction, knowing that we are getting closer to the transus  $\beta$  temperature, the dissolution of the  $\alpha$  has largely started.

**$\beta$  phase fraction as a function of temperature.** To analyze the influence of the temperature on the  $\alpha$  grain size growth and on the  $\beta$  phase fraction, heat treatments are done at  $750^\circ\text{C}$ ,  $870^\circ\text{C}$  and  $920^\circ\text{C}$ . The Fig. 4 shows SEM microstructures obtained after heat treatment at  $750^\circ\text{C}$ ,  $870^\circ\text{C}$  and  $920^\circ\text{C}$ . As previously explained for samples water quenched from temperatures included in the range of the  $\alpha \rightarrow \beta$  transformation, at room temperature it can be observed a martensitic  $\alpha'$  in grey and lathlike while the  $\alpha$  and the  $\beta$  phases appear respectively in black and white. The Fig.4-a shows that after the heat treatment at  $750^\circ\text{C}$ , only the  $\alpha$  and the  $\beta$  phases are detected as well as a spheroidization of  $\alpha$  grains. Because no martensite can be clearly revealed it can be conclude that at  $750^\circ\text{C}$  the dissolution of  $\alpha$  has not already started. On the contrary, after heat treatment at  $870^\circ\text{C}$  and  $920^\circ\text{C}$  the martensite, which can be directly linked to the proportion of  $\beta$  at high temperature, is shown in grey respectively on Fig. 4b and 4c. So the  $\beta$  volume proportion increases from 13% at  $750^\circ\text{C}$  to approximately 61% at  $920^\circ\text{C}$ . This is in accordance with the study of Elmer et al. who found that it is only around  $850^\circ\text{C}$  that the phase transformation should begin [11] as well as with the work of Malinov [12]. It can be also noticed that by increasing the temperature, the number of  $\alpha$  grains decreases for the same surface analyzed and so a grain growth occurs. At  $920^\circ\text{C}$  due to the high  $\beta$  phase fraction (61%), a change in the (super)plastic deformation mechanisms can be admissible. While at lower temperature (and so for a lower  $\beta$  phase fraction) and as proposed recently by Alabort [5], the superplastic mechanism could be explained by  $\alpha$  GBS associated by several accommodation mechanisms (in particular in the  $\beta$  phase). According to Alabort, depending on the temperature, the  $\alpha$ -GBS would be the major deformation mechanism with, in addition, intragranular deformation in  $\alpha$ , visible by the accumulation of dislocations at grain boundaries leading to the recrystallization of  $\alpha$  grains. Moreover, the intergranular deformation in  $\alpha$  appears to decrease with increasing temperature [5]. It appears that the  $\beta$  fraction around 60%, can induce modifications of the nature and number of interfaces/boundaries ( $\alpha/\alpha$  and/or  $\beta/\alpha$  and/or  $\beta/\beta$ ) and so to probably interfere with the grain boundary sliding mechanism as well as with the accommodation mechanisms.

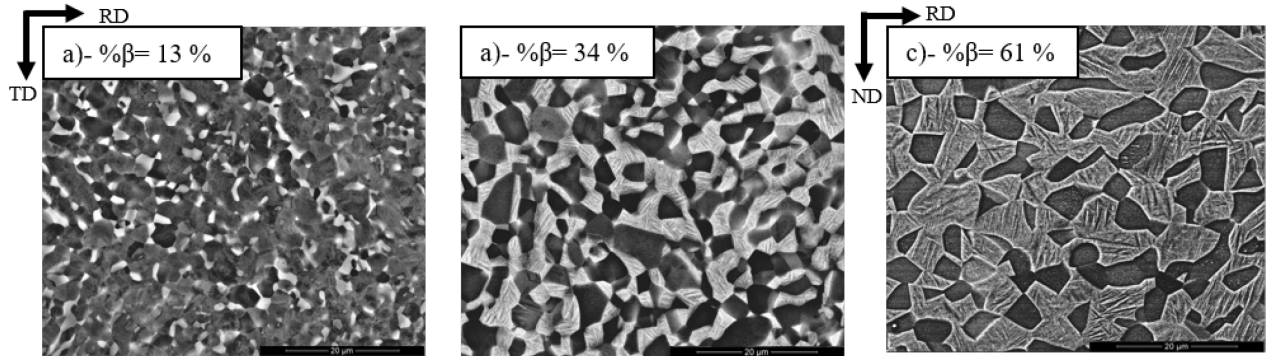


Fig. 4: Microstructural observations after heat treatment to 750°C (a), 870°C (b) and 920°C (c) by SEM with CBS (x2000).

**Interrupted tensile tests.** Fig 5a shows the stress strain response obtained at 920°C for a strain rate of  $10^{-4} \text{ s}^{-1}$  and for 200%, 400% and 800% of deformation. Firstly these interrupted tensile tests showed that the strain-stress response, characterized by a pronounced flow hardening, are reproducible (Fig.5). As the samples were cooled down slowly in the furnace after the tensile tests, the grain size evolution is not interpreted here.

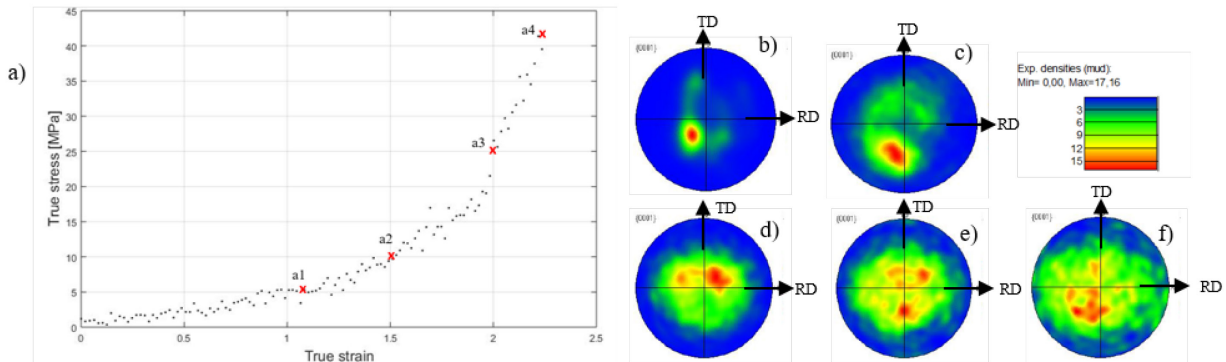


Fig. 5: True stress-true strain curve corresponding to tensile tests at 920°C with a strain rate of  $10^{-4} \text{ s}^{-1}$  on initial grain size about  $3 \mu\text{m}$  (a). Points a1, a2, a3 correspond respectively to interrupted samples at 110%, 150%, 200% of true strain and the point a3 to the end of the test. {0002} pole figures obtained by EBSD in the  $\alpha$  phase for the initial state (b), after interrupted tensile tests at 110% (c), 150% (d), 200% (e) of true strain and at the end of the test (f).

Meanwhile a particular interest will be done on the orientation of grains. Figure 5-b to f show the basal poles {0002} from the  $\alpha$  phase obtained by EBSD before and after the four interrupted tensile tests (200%, 400%, 800% of deformation and at the end of the test). As already presented (Fig. 1b), the initial sample is characterized by a preferred orientation of the  $\alpha$  grain (Fig. 5-a). When the sample is deformed on superplastic conditions, we can expect the loss of texture due to the grain boundary sliding deformation mechanism [13-14]. But in Fig. 5-d) and -e), the texture is not really lost. It is admitted that a dramatic decrease in texture intensity is explained by non-crystallographic grain rotation due to grain boundary sliding. Here a slight decrease of the texture intensity is observed revealing the occurrence of grain boundary sliding but only to a lesser extent. Thus observations highlight that an accommodation mechanism could have a role into the deformation in this case, with the experimental conditions: 920°C and  $10^{-4} \text{ s}^{-1}$ . Different type of accommodation mechanisms exist, such as the accommodation by diffusion or by dislocations slip [5] or also by stress-phase transformation  $\alpha$  to  $\beta$  [15]. Looking at the evolution of the curve that undergoes hardening at a high deformation rate, conventional superplasticity no longer seems to occur. This behavior could be due to the proportion of  $\beta$  that has greatly increased as well as to the distribution of the phase which is different. Indeed, as we have seen previously, at lower temperature, the  $\beta$  phase is distributed around the grains in the form of fine edging and the deformation mechanism is GBS [5]. Whereas at higher temperatures, the  $\beta$  phase seems to be distributed in the form of

equiaxed grains. So the grain growth associated to this new repartition and morphology of beta could explain the high hardening observed on the stress-strain response at 920°C. Indeed we could assume a lower occurrence of the GBS mechanism, due to the decrease of the “ $\alpha$ /thin- $\beta/\alpha$ ” interfaces, in favor of another mechanism mainly occurring in the  $\beta$  phase. For example, as proposed by Alabort et al., for a temperature of 900°C, the GBS would be completed by the dislocations slip confined in  $\beta$ , which has all the more influence as the temperature is high [5]. Therefore another unknown type of deformation could play a role into the deformation. For the  $\beta$  phase, the texture is also partially maintained. However none assumption can be made on the evolution of the  $\beta$  texture because the number of grains analyzed is insufficient and so the statistics is not good enough. It seems important in future works to go deeper into the influence of the  $\beta$  phase.

## Summary

Several items were investigated. Firstly the flow stress in the titanium Ti-6Al-4V alloy was studied for a wide range of temperatures (750°C-920°C) and strain rates ( $10^{-2} \text{ s}^{-1}$ - $10^{-4} \text{ s}^{-1}$ ). The flow behavior exhibits a pronounced flow-hardening at 920°C- $10^{-4} \text{ s}^{-1}$  that cannot be explained only by a grain growth phenomena. Secondly the  $\beta$  phase fraction was shown to rise from 870°C. Then the texture evolution after interrupted tensile tests (200%, 400% and 800% of deformation) carried out at 920°C and with a strain rate of  $10^{-4} \text{ s}^{-1}$  was obtained by XRD and EBSD.

It shows that the initial state is textured, whether it is for the  $\alpha$  or for the  $\beta$  phase. After deformation at 920°C- $10^{-4} \text{ s}^{-1}$ , the  $\alpha$  phase seems to keep a part of the texture revealing that not only the mechanism of GBS is activated. In particular the high hardening could be due to the grain growth but also to the decrease of the “ $\alpha$ /thin- $\beta/\alpha$ ” interfaces number. This feature combined to the high fraction of the  $\beta$  phase could lead to the occurrence of another mechanism as dislocation slip into  $\beta$ . For this phase, complementary analyses are needed. So the information on texture obtained allow to keep the same conclusion that the grain boundary sliding is maybe the predominant deformation mechanism but there are most probably complementary accommodation mechanisms, in particular in the beta phase, like diffusion or crystallographic slip and why not a stress-phase transformation of  $\alpha$  to  $\beta$  accommodation mechanism.

## References

- [1] S. Semiatin and T. Bieler, The effect of alpha platelet thickness on plastic flow during hot working of Ti-6Al-4V with a transformed microstructure, *Acta Mater.* Vol.49 (2001) 3565-3573.
- [2] S. V. Zharebtsov, E. A. Kudryavtsev, G. A. Salishchev, B. B. Straumal, and S. L. Semiatin, Microstructure evolution and mechanical behavior of ultrafine Ti6Al4V during low-temperature superplastic deformation, *Acta Mater.* Vol.121 (2016) 152-163.
- [3] H. Matsumoto, V. Velay and A. Chiba, Superplasticity of the Ultrafine-Grained Ti-6Al-4V Alloy with a Metastable  $\alpha$ -Single Phase Microstructure, in *Proceedings of the 13th World Conference on Titanium* (eds V. Venkatesh, A. L. Pilchak, J. E. Allison, S. Ankem, R. Boyer, J. Christodoulou, H. L. Fraser, M. A. Imam, Y. Kosaka, H. J. Rack, A. Chatterjee and A. Woodfield), John Wiley & Sons, Inc., Hoboken, NJ, USA (2016).
- [4] M. Ashby, R. Verrall, Diffusion-accommodated flow and superplasticity, *Acta Metall.* 21 (1973) 149-163.
- [5] E. Alabort, P. Kontis, D. Barba, K. Dragnevski, and R. C. Reed, On the mechanisms of superplasticity in Ti-6Al-4V, *Acta Mater.* Vol.105 (2016) 449-463.
- [6] Velay, V., Matsumoto, H., Sasaki, L. and Vidal, V., Investigation of the mechanical behaviour of Ti-6Al-4V alloy under hot forming conditions, *Mat.-wiss. u. Werkstofftech.* Vol.45 (2014) 847-853.
- [7] V. Velay, H. Matsumoto, V. Vidal, and A. Chiba, Behavior modeling and microstructural evolutions of Ti-6Al-4V alloy under hot forming conditions, *International Journal of Mechanical Sciences.* Vol.108-109 (2016) 1-13.

- [8] H. S. Yang, G Gurewitz and A. K. Mukherjee, Mechanical Behavior and Microstructural Evolution during Superplastic Deformation of Ti-6Al-4V, *Materials Transactions*, Vol.32 (1991) 465-472
- [9] P. M. Souza, H. Beladi, R. Singh, B. Rolfe, and P. D. Hodgson, Constitutive analysis of hot deformation behavior of a Ti6Al4V alloy using physical based model, *Materials Science and Engineering*. Vol.648 (2015) 265–273.
- [10] J. J. Jonas, C. Aranas, A. Fall, and M. Jahazi, Transformation softening in three titanium alloys, *Materials & Design*. Vol.113 (2017) 305–310
- [11] J. W. Elmer, T. A. Palmer, S. S. Babu, and E. D. Specht, In situ observations of lattice expansion and transformation rates of  $\alpha$  and  $\beta$  phases in Ti–6Al–4V, *Materials Science and Engineering*, Vol.391 (2005) 104–113.
- [12] S. Malinov, P. Markovsky, W. Sha, and Z. Guo, Resistivity study and computer modelling of the isothermal transformation kinetics of Ti–6Al–4V and Ti–6Al–2Sn–4Zr–2Mo–0.08Si alloys, *Journal of Alloys and Compounds*. Vol.314 (2001) 181-192.
- [13] F. A. Mohamed, Micrograin Superplasticity: Characteristics and Utilization, *Materials*, Vol.4 (2011).
- [14] E. Alabort, D. Putman, and R. C. Reed, Superplasticity in Ti–6Al–4V: Characterisation, modelling and applications, *Acta Mater*. Vol.95 (2015) 428–442.
- [15] J. Koike *et al.*, Stress-induced phase transformation during superplastic deformation in two-phase Ti–Al–Fe alloy, *Acta Mater*. Vol.48 (2000) 2059–2069.